High-order cumulants of wolfram metal in anharmonic EXAFS theory calculated using the correlated Einstein model

Nguyen To Nu[1], Nguyen Huy Thao[2], Nguyen Thi Minh Thuy[3], Tong Sy Tien[3*]

[1]Phong Chau High School, Lam Thao Department of Education, Phu Tho, Vietnam;
[2]Department of Physics, Hanoi Pedagogical University 2, Vinh Phuc, Vietnam;
[3]Faculty of Fundamental Sciences, University of Fire Prevention and Fighting, 243 Khuat Duy Tien, Thanh Xuan, Hanoi, Vietnam.
[*]Corresponding author: tongsytien@yahoo.com
Received 04 Mar. 2025; Revised 29 Apr. 2025; Accepted 09 May 2025; Published 25 May 2025.
DOI: https://doi.org/10.54939/1859-1043.j.mst.103.2025.82-91

ABSTRACT

The anharmonic extended X-ray absorption fine structure (EXAFS) cumulants of wolfram metal (W) in expansion to the 4th order have been calculated under the influence of thermal disorder. The temperature-dependent EXAFS cumulants were calculated explicitly and simply from a theoretical model developed based on the anharmonic effective potential and classical *statistical theory within the correlated Einstein model. The thermodynamic parameters of W have been considered the influence of the nearest neighbor atoms on the backscattering and absorbing atoms. The obtained numerical results of W at temperatures from 0 to 800 K fit with* those *obtained* from the *experimental EXAFS data and the anharmonic correlated Debye (ACD) model at various temperatures. These results indicate that the* present *theoretical model can helpfully analyze experimental EXAFS signals of W and other similar metals.*

Keywords: High-order EXAFS cumulants; Thermal disorder; Wolfram metal; Classical statistics; Correlated Einstein model.

1. INTRODUCTION

Nowadays, many of the thermodynamic properties and structural parameters of materials can be identified using the extended X-ray absorption fine structure (EXAFS) analysis [1]. The information on thermal vibrations can be extracted from fitting theoretical EXAFS signals to experimental EXAFS signals via several defined parameters [2]. However, the thermal disorder is sensitive to EXAFS oscillations and causes anharmonic effects [3], as seen in figure 1. It is observable that the anharmonicity of the EXAFS oscillation is significant, as observed via the peak shifts and their heights [4], so the thermal disorder should be considered in the EXAFS signal analysis.

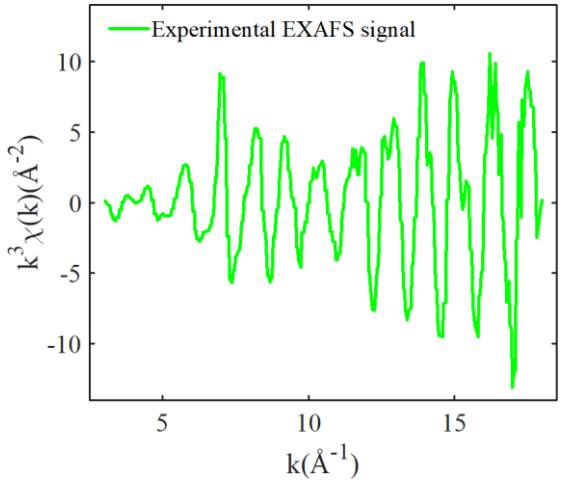

Figure 1. *The EXAFS signal of W at 573 K is obtained from the experimental data [4].*

Nowadays, the wolfram metal (W) has the advantages of high melting point, high hardness, excellent corrosion resistance, and good electrical and thermal conductivity and is alloyed with other metals to strengthen them [5], so this metal and its alloys are used in many high-tech applications, such as lighting filaments, electronic contacts, wire, rods, heating elements, arc-welding electrodes, and magnetrons for microwave ovens. [6]. Meanwhile, the experimental EXAFS cumulants of W at seven points from room temperature to 573 K were measured at the Synchrotron Radiation Siberian Center (SRSC), Russia, by Nedoseikina & Pirog *et al.* [4].

Recently, in analyzing the anharmonic EXAFS signal of metals, some suitable theoretical models have been developed using suitable statistical theories based on the correlated Debye (CD) and correlated Einstein (CE) models [7-10]. The CE model uses only one effective frequency to describe thermal vibrations in crystals, so it cannot describe the acoustic phonon branch, whereas the CD model can consider the phonon-dispersion effect with variable frequencies, so it has the advantage of being able to describe the acoustic phonon branch in crystals effectively. Each model has its own disadvantages and advantages in the anharmonic EXAFS data analysis. A theoretical model has been derived from combining the anharmonic effective (AE) potential and classical statistical theory with the correlated Einstein model (hereinafter referred to as the CACE model) [7]. This model has been developed to effectively process the EXAFS cumulants of metals by Hung *et al.* and Tien *et al.* [8]. The CACE model is very convenient for analyzing the anharmonic EXAFS cumulants because it allows temperature-dependent EXAFS cumulants to be expressed in simple and explicit forms [9]. Still, it has not yet been applied to analyze the high-order EXAFS cumulants of W under the influence of thermal disorder. Also, another theoretical model has been used in the anharmonic EXAFS data analysis of W, which is the anharmonic correlated Debye (ACD) model that can consider both the phonon dispersion relations and the anharmonic and quantum effects simultaneously [10]. Still, it is not convenient for analyzing anharmonic EXAFS cumulants because it allows temperature-dependent EXAFS cumulants to be expressed in very complex forms, in which the 1st, 2nd, and 4th EXAFS cumulants have not been performed in numerical calculations yet. However, the limitation of the ACD model is that the anharmonic EXAFS cumulants are not obtained in explicit expressions, so it takes a lot of computational effort to perform the anharmonic EXAFS data analysis. Hence, analyzing high-order anharmonic EXAFS cumulants of W using the CACE model will be essential to optimize the analytical technique of the experimental EXAFS data.

2. FORMALISM AND CALCULATION MODEL

Normally, the cumulant expansion approach is used to describe anharmonic EXAFS oscillations [11]. The formalism of the EXAFS function, including anharmonic effects for a single coordination shell, can be represented within the framework of the plane-wave approximations and single-scattering as follows [12]:

$$\chi(k) = F(k)\frac{e^{-2R/\lambda(k)}}{kR^2}\,\mathrm{Im}\left\{e^{i\phi(k)}\exp\left[2ikR + \sum_n \frac{(2ik)^n}{n!}\sigma^{(n)}\right]\right\}, \quad (1)$$

where $\sigma^{(n)}$ is the nth order cumulant, $F(k)$ is the atomic backscattering amplitude, $R = \langle r \rangle$ is the average interatomic distance with $\langle\ \rangle$ denotes the thermal average and r is the instantaneous interatomic distance, k is the photoelectron wavenumber, $\phi(k)$ is a net phase shift, and $\lambda(k)$ is the electron mean free path of photoelectrons.

In the cumulant expansion approach, the accuracy of anharmonic EXAFS data analysis can be improved by extending the anharmonic EXAFS signal in approximation up to the 4th order [11].

The low-order moments of the radial pair distribution (RPD) function $\rho(r,T)$ are directly linked to the temperature-dependent EXAFS cumulants [13], so they can be used to express the first four EXAFS cumulants in analyzing the anharmonic EXAFS data as follows [12]:

$$\sigma^{(1)} = \langle r \rangle - r_0 = \langle x \rangle, \tag{2}$$

$$\sigma^{(2)} \equiv \sigma^2 = \left\langle \left(r - \langle r \rangle \right)^2 \right\rangle = \left\langle x^2 \right\rangle - \langle x \rangle^2, \tag{3}$$

$$\sigma^{(3)} = \left\langle \left(x - \langle x \rangle \right)^3 \right\rangle = \left\langle x^3 \right\rangle - 3\left\langle x^2 \right\rangle \langle x \rangle + 2\langle x \rangle^3, \tag{4}$$

$$\sigma^{(4)} = \left\langle \left(x - \langle x \rangle \right)^4 \right\rangle - 3\left[\left\langle \left(x - \langle x \rangle \right)^2 \right\rangle \right]^2 = \left\langle x^4 \right\rangle + 12\left\langle x^2 \right\rangle \langle x \rangle^2 - 3\left\langle x^2 \right\rangle^2 - 4\left\langle x^3 \right\rangle \langle x \rangle - 6\langle x \rangle^4, \tag{5}$$

where $x = r - r_0$ is the deviation interatomic distance from the equilibrium position, and cumulants $\sigma^{(1)}$, $\sigma^{(2)}$, $\sigma^{(3)}$, and $\sigma^{(4)}$ describes the centroid, variance, asymmetry, and flatness of the RPD function, respectively.

Usually, the PI potential of metals can be validly identified using the Morse potential with α characterizes the potential width and *D* is the dissociative energy, it is written in the form [14]:

$$\varphi(x) = D\left(\mathrm{e}^{-2\alpha x} - 2e^{-\alpha x} \right), \tag{6}$$

This potential can be written in expanding up to the 4th-order approximation around its minimum position:

$$-D + D\alpha^2 x^2 - D\alpha^3 x^3 + 7D\alpha^4 x^4 / 12, \tag{7}$$

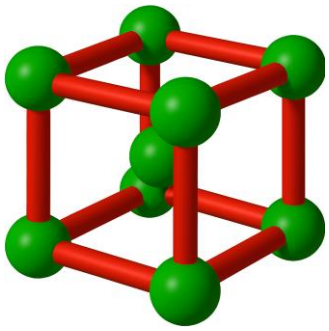

Figure 2. *The structural model of W.*

The crystalline structure of W is illustrated in figure 2, which has similar atoms with eight atoms at each corner and one center of a cube, so this structure is a body-centered cubic (BCC), with each unit cell containing two atoms [15].

Normally, one needs to determine the AE potential from the atomic interaction (AI) potential of the single bond (SB) pairs in the crystal lattice, which is used to identify the thermodynamic parameters of the system [7]. The AE potential in the relative vibrations of backscattering (*B*) and absorbing (*A*) atoms can be calculated using the pair interaction (PI) potential [16]:

$$V_{eff} = \varphi(x) + \sum_{i=A,B} \sum_{j \neq A,B} \varphi\left(\varepsilon_i x \hat{R}_{AB} \hat{R}_{ij} \right), \ \varepsilon_i = \frac{\mu}{M_i}, \tag{8}$$

where $\hat{R}$ is the bond unit vector**,** sum *i* is the over backscattering and absorbing atoms, the sum *j* is over all their nearest neighbors, $\mu = M_A M_B / (M_A + M_B)$ is the reduced mass of a single bond pair with atomic masses M_A and M_B, $\varphi(x)$ is a PI potential of backscattering and absorbing

atoms, $\varphi\left(\varepsilon_i x\hat{R}_{AB}\hat{R}_{ij}\right)$ is the nearest-neighbor atomic contributions and characterizes the correlation effect caused by these atoms on the PI potential.

After using structural characteristics, the AE potential of W is obtained by equation (8) and is presented as:

$$V_{eff}(x)=\varphi(x)+\varphi(0)+2\varphi\left(-\frac{1}{2}x\right)+6\varphi\left(-\frac{1}{6}x\right)+6\varphi\left(\frac{1}{6}x\right), \tag{9}$$

The result of AE potential can be obtained from equation (8) using Morse potential in equation (7). After ignoring the constant contribution in the approximate expansion to the 4th order, the AE potential can be presented in the form [12]:

$$V_{eff}(x)=\frac{1}{2}k_{eff}x^2-k_3x^3+k_4x^4, \tag{10}$$

where k_{eff} is an effective force constant, k_3 and k_4 are the anharmonic force constants, which are not temperature-dependent and are written as:

$$k_{eff}=\frac{11}{3}D\alpha^2,\quad k_3=\frac{3}{4}D\alpha^3,\quad k_4=\frac{1715}{2592}D\alpha^4, \tag{11}$$

In the CACE model, each atomic thermal vibration can be processed as a phonon and characterized via the correlated Einstein frequency ω_E and temperature θ_E [7]. Utilizing the effective force constant, these parameters of W can be defined as follows:

$$\omega_E=\sqrt{\frac{k_{eff}}{\mu}}=\alpha\sqrt{\frac{22D}{3m}}, \tag{12}$$

$$\theta_E=\frac{\hbar\omega_E}{k_B}=\frac{\hbar\alpha}{k_B}\sqrt{\frac{22D}{3m}}, \tag{13}$$

where k_B is the Boltzmann constant and $\hbar$ is the reduced Planck constant.

In the classical statistical theory processed by Stern *et al*., the moments $\langle x^k\rangle$ can be identified from the 3rd-order approximation of the thermal average [17]:

$$\langle x^k\rangle=\frac{\int_{-\infty}^{\infty}x^k\exp\left[-\frac{V_{eff}(x)}{k_BT}\right]dx}{\int_{-\infty}^{\infty}\exp\left[-\frac{V_{eff}(x)}{k_BT}\right]dx}\approx\frac{\int_{-\infty}^{\infty}x^k\exp\left(\frac{-k_{ef}x^2}{2k_BT}\right)\left\{\sum_{n=0}^{3}\frac{1}{n!}\left(\frac{k_3x^3-k_4x^4}{k_BT}\right)^k\right\}dx}{\int_{-\infty}^{\infty}\exp\left(\frac{-k_{eff}x^2}{2k_BT}\right)\left\{\sum_{n=0}^{3}\frac{1}{n!}\left(\frac{k_3x^3-k_4x^4}{k_BT}\right)^k\right\}dx}. \tag{14}$$

Utilizing equations (2)-(5) to calculate anharmonic EXAFS cumulants in the temperature dependence based on equation (14) in the CACE model, we obtain the following result:

$$\sigma^{(1)}\simeq\frac{81k_BT}{484D\alpha}\left(1-\frac{203425k_BT}{191664D}\right)\approx\frac{81k_BT}{484D\alpha}, \tag{15}$$

$$\sigma^{(2)}\simeq\frac{3k_BT}{11D\alpha^2}\left(1-\frac{5743k_BT}{31944D}\right)\approx\frac{3k_BT}{11D\alpha^2}, \tag{16}$$

$$\sigma^{(3)}\simeq\frac{243(k_BT)^2}{2662D^2\alpha^3}\left(1-\frac{79567k_BT}{31944D}\right)\approx\frac{243(k_BT)^2}{2662D^2\alpha^3}, \tag{17}$$

$$\sigma^{(4)} \simeq \frac{12270\left(k_B T\right)^3}{322102\, D^3 \alpha^4}\left(1+\frac{3975025253 k_B T}{69680512\, D}\right) \approx \frac{12270\left(k_B T\right)^3}{322102\, D^3 \alpha^4}. \quad (18)$$

Thus, the temperature-dependent EXAFS cumulants of W have been efficiently calculated under the influence of thermal disorder by extending the CACE model. The obtained expressions are in simple and explicit forms, and they can meet all basic properties in temperature dependence, in which cumulants $\sigma^{(1)}$ and σ^2, $\sigma^{(3)}$, and $\sigma^{(4)}$ are proportional to T, T^2, and T^3, respectively. These expressions show the influence of anharmonic effects on the classical limit at high temperatures and indicate that the analytic expressions of high-order EXAFS cumulants are very helpful for processing the anharmonic EXAFS signals.

3. RESULTS AND DISCUSSIONS

In this section, the obtained expressions in Sec. 2 are used to calculate the numerical results of W based on its basic physical parameters. The calculations use Morse potential parameters $D = 0.9906$ eV, $\alpha = 1.4116$ Å^{-1}, and $r_0 = 3.032$ Å identified by Girifalco & Weizer [14]. The obtained numerical results of the anharmonic EXAFS cumulants are determined at temperatures from 0 to 800 K. Our obtained results from the present CACE model are compared with those obtained from the ACD model [10] and an experiment [4]. Herein, the obtained EXAFS cumulants from the ACD model are calculated based on the temperature-dependent expressions reported in Ref. 10, while the experimental EXAFS cumulants at 293 K, 323 K, 373 K, 423 K, 473 K, 523 K, and 573 K are performed by Nedoseikina & Pirog at the SRSC, Russia [4]. The numerical results are presented below.

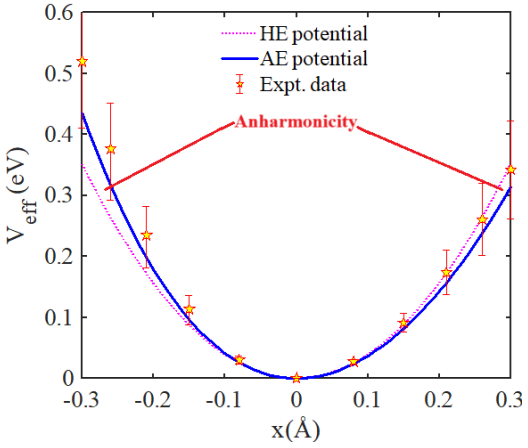

Figure 3. *The position-dependent AE and harmonic effective (HE) potentials of W are obtained from the present CACE model and experimental data [4].*

The local force constants k_{eff}, k_3, and k_4, and correlated Einstein frequency ω_E and temperature θ_E can describe the power of atomic thermal vibrations, which are calculated by equations (11)-(13) with the atomic mass $m = 183.85$ u reported by Ashcroft & Mermin [18]. Our calculated results from the present CACE model obtained are $k_{eff} \simeq 7.24$ eVÅ^{-2}, $k_3 \simeq 2.09$ eVÅ^{-3}, $k_4 \simeq 2.60$ eVÅ^{-4}, $\theta_E \simeq 209.92$ K, and $\omega_E \simeq 2.75\times10^{13}$ Hz. Meanwhile, the respective values obtained from the experiment are $k_{eff} \simeq 9.5 \pm 0.9$ eVÅ^{-2}, $k_3 \simeq 3.5 \pm 0.8$ eVÅ^{-3}, $k_4 \simeq 3.8 \pm 4.7$ eVÅ^{-4}, $\omega_E \simeq 2.8 \pm 0.2 \times 10^{13}$ Hz, and $\theta_E \simeq 214.0 \pm 12.0$ K [4]. It should be noted that the present CACE and ACD models both use the same AE potential with the same local force constants. It is

observable that our results are consistent with the experimental values in error ranges, especially for the correlated Einstein temperature and frequency.

The AE and HE potentials of W at positions from - 0.3 to 0.3 Å are illustrated in figure 3. Our obtained result from the present CACE model is calculated by equations (10)-(11) with the above force constants. Herein, the AE potential takes into account 4th-order terms, and the HE potential only takes into account 2nd-order terms in equation (10). Meanwhile, the experimental results of the AE potential are obtained by equation (10) with experimental force constants given above. It is observable that our AE potential result fits with those obtained from the experimental data with error bars. Moreover, the obtained results indicate that the plot presenting the asymmetry of the AE potential, in which values at negative positions (x < 0) are bigger than those at the positive positions (x > 0) of the same magnitude, as seen in figure 3.

Table 1. *The AE and HE potentials of W are obtained from the present CACE model and experimental data.*

Quantity	**Value**										
x (Å)	- 0.30	- 0.26	- 0.21	- 0.15	- 0.08	0	0.08	0.05	0.10	0.15	0.30
V_{eff} (eV)[a]	0.35	0.26	0.17	0.09	0.03	0	0.03	0.09	0.17	0.26	0.35
V_{eff} (eV)[a]	0.44	0.32	0.20	0.10	0.03	0	0.02	0.08	0.16	0.28	0.31
V_{eff} (eV)[b]	0.52 ± 0.10	0.38 ± 0.08	0.23 ± 0.05	0.11 ± 0.02	0.03 ± 0.01	0	0.03 ± 0.01	0.09 ± 0.02	0.17 ± 0.04	0.26 ± 0.06	0.34 ± 0.08

[a]*The HE potential is obtained from the present CACE model.*
[b]*The AE potential is obtained from the present CACE model.*
[c]*The AE potential is obtained from experimental data [4].*

The values of the AE and HE potentials of W obtained from the present CACE model and experimental data are given in table 1. It is observable that the further from the equilibrium position, the AE potential is influenced more strongly by the anharmonic effect caused by terms $(-k_3x^3)$ and (k_4x^4). The thermal disorder has a significant effect when it causes a strong enough anharmonic effect to change the atomic positions in the crystal significantly. Hence, its effect on the AE potential shows clear anharmonicity in the temperature range above the correlated Einstein temperature, as seen in table 1.

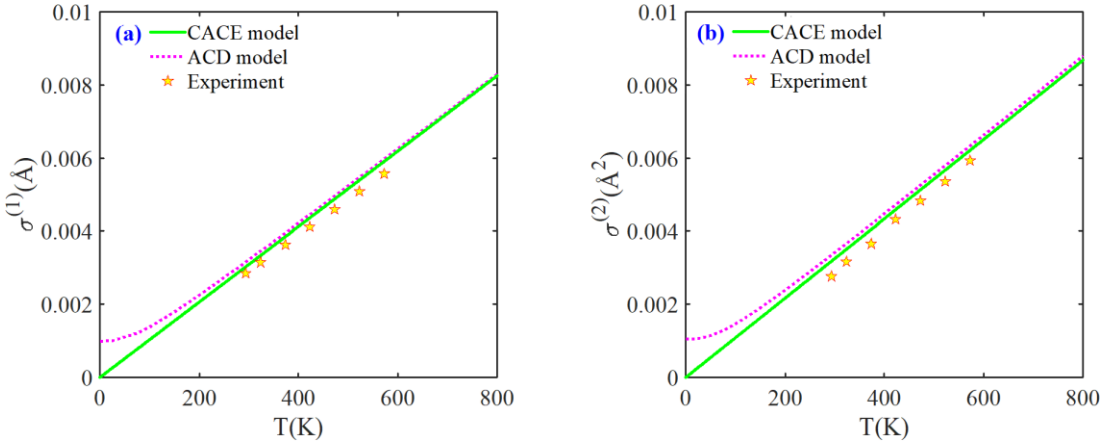

Figure 4. *The temperature-dependent of the (a) 1st and (b) 2nd cumulants of W are obtained using the present CACE model, ACD model [10], and experiment [4].*

The (a) 1st cumulant $\sigma^{(1)}(T)$ and (b) 2nd cumulant $\sigma^{2}(T)$ of W at temperatures from 0 to 800 K are illustrated in figure 4. Our obtained results using the present CACE model are calculated by equations (15)-(16). It is observable that our results fit with those obtained from the ACD model [10] and experiment [4] in the high-temperature (HT) range. Our results are zero as the temperature goes to the zero-point (ZP) because the present CACE model only uses a classical statistical theory and cannot calculate quantum effects like the ACD model [10]. The present CACE model cannot work well in the low-temperature (LT) range. Still, it works correctly at room temperature, especially at temperatures higher than the correlated Einstein temperature θ_E, as seen in figure 4.

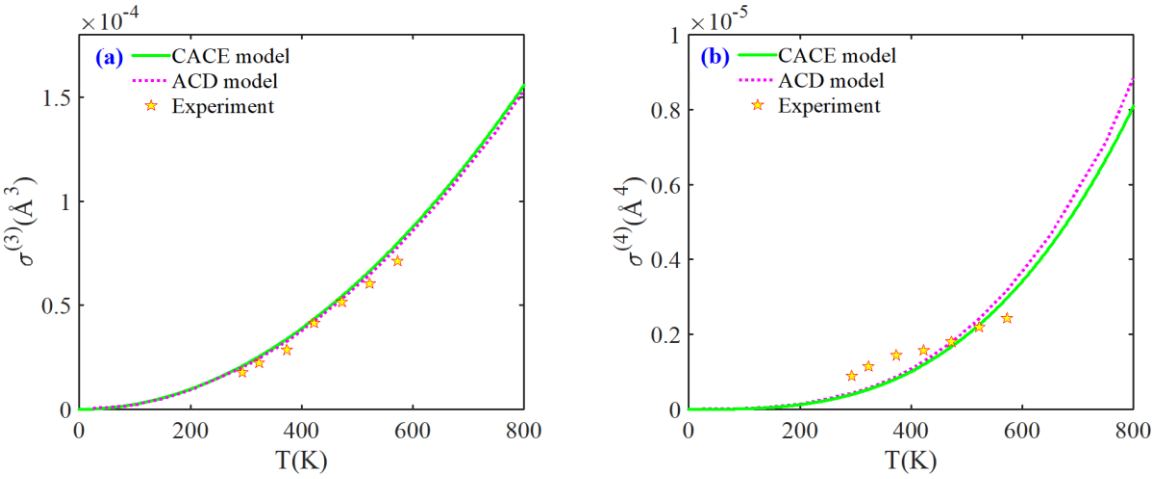

Figure 5. *The temperature-dependent of the (a) 3rd and (b) 4th cumulants of W are obtained from the present CACE model, ACD model [10], and experiment [4].*

The (a) 3rd cumulant $\sigma^{(3)}(T)$ and (b) 4th cumulant $\sigma^{(4)}(T)$ of W at temperatures from 0 to 800 K are illustrated in figure 5. Our obtained results from the present CACE model are calculated by equations (17)-(18). It is observable that our results fit well with those obtained from the ACD model [10] and experiment [4], especially at not-too-low temperatures. However, the present CACE model still works well for 3rd and 4th order cumulants in the LT range. This is because the contribution of quantum effects is negligible to the high-order cumulants at low temperatures, while the anharmonic effect is more evident. Moreover, the present CACE model obtains small results and is not suitable at low temperatures in comparison with the obtained results from the ACD model [10] and experiment [4]. However, low-order EXAFS cumulants still agree well at temperatures ranging from above θ_E to just before the melting point, whereas the high-order EXAFS cumulants can be satisfied at temperatures ranging from above $\theta_E/2$ to just before the melting point, as seen in figure 5.

The values of the EXAFS cumulants of W at several temperatures are given in table 2. The relative mean square error (RMSE) for each EXAFS cumulant of W is calculated by comparing the values obtained from the present CACE and ACD [10] models with the corresponding experimental values [4]. The RMSEs of the first four EXAFS cumulants of W obtained from the present CACE and ACD models are $RMSE_{\sigma^{(1)}} \approx 0.26\times10^{-3}$ Å, $RMSE_{\sigma^{(2)}} \approx 0.77\times10^{-3}$ Å^2, $RMSE_{\sigma^{(2)}} \approx 0.53\times10^{-5}$ Å^3, and $RMSE_{\sigma^{(2)}} \approx 0.46\times10^{-6}$ Å^4 and $RMSE_{\sigma^{(1)}} \approx 0.37\times10^{-3}$ Å [10], $RMSE_{\sigma^{(2)}} \approx 0.87\times10^{-3}$ Å^2 [10], $RMSE_{\sigma^{(2)}} \approx 0.43\times10^{-5}$ Å^3 [10], and $RMSE_{\sigma^{(2)}} \approx 0.44\times10^{-6}$ Å^4 [10], respectively. It is observable that our obtained values of $RMSE_{\sigma^{(1)}}$ and $RMSE_{\sigma^{(2)}}$ are

smaller than those obtained from the ACD model, whereas the obtained values of $RMSE_{\sigma^{(3)}}$ and $RMSE_{\sigma^{(4)}}$ are bigger in similar comparisons. This is because higher-order EXAFS cumulants have smaller and smaller values, causing quantum effects to contribute more and more to their values, as seen in table 2.

Table 2. *The EXAFS cumulants of W are obtained from the present CACE model, ACD model, and experiment.*

Method	T (K)	$\sigma^{(1)}$ ($\times 10^{-3}$ Å)	$\sigma^{(2)}$ ($\times 10^{-3}$ Å^2)	$\sigma^{(3)}$ ($\times 10^{-5}$ Å^3)	$\sigma^{(4)}$ ($\times 10^{-6}$ Å^4)
CACE model [a]	293	3.0	3.4	2.1	0.4
	323	3.3	3.8	2.5	0.5
	373	3.8	4.4	3.4	0.8
	423	4.4	5.0	4.3	1.2
	473	4.9	5.6	5.4	1.7
	523	5.4	6.2	6.6	2.3
	573	5.9	6.7	8.0	3.0
ACD model [d]	293	3.2	3.6	2.0	0.4
	323	3.4	3.9	2.5	0.6
	373	3.9	4.5	3.3	0.9
	423	4.5	5.1	4.2	1.3
	473	5.0	5.7	5.3	1.8
	523	5.5	6.2	6.5	2.4
	573	6.0	6.8	7.8	3.1
Experiment [e]	293	2.8	2.7	1.7	0.9
	323	3.1	3.1	2.1	1.1
	373	3.6	3.6	2.8	1.4
	423	4.1	4.3	4.1	1.6
	473	4.6	4.8	5.1	1.8
	523	5.1	5.3	6.0	2.2
	573	5.6	5.9	7.1	2.4

[a]*Our obtained values are calculated from the present CACE model.*
[d]*The obtained values are calculated from the ACD model [10].*
[e]*The obtained values are measured from the experiment [4].*

Thus, the first four EXAFS cumulants of W are obtained from the present CACE model, which can satisfy fundamental properties in comparison with the ACD model and experiment at not-too-low temperatures, particularly above the correlated Einstein temperature. These results describe thermal vibration contributions influencing the classical limit via anharmonic effects at high temperatures, in which the anharmonicity of the EXAFS signal arises from above θ_E, even at room temperature.

4. CONCLUSIONS

In this work, we have effectively applied the present CACE model to calculate the temperature-dependent high-odder EXAFS cumulants of W under the influence of thermal disorder. The obtained expressions of the first four EXAFS cumulants are in simple and explicit forms of the temperature *T*. These results can meet all basic properties in the temperature dependence and show the anharmonicity of the EXAFS signal at high temperatures, in which the 1st, 2nd, 3rd, and 4th EXAFS cumulants are proportional to T, T^2, and T^3, respectively. Our numerical results of W fit with those obtained from the ACD model and experiment at high temperatures, even at room temperature, particularly for high-order cumulants. The agreement between our results and other results in the comparisons indicates the usefulness of this calculation model. This model can be applied to analyze experimental EXAFS cumulants of other similar metals with BCC structure (such as Fe, Cu, and Mo) from above the temperature θ_E to just before the melting point.

Acknowledgments: *This research is funded by the Vietnam National Foundation for Science and Technology Development (NAFOSTED) under grant number 103.01-2023.32*.

REFERENCES

[1]. C. W. Pao et al., "*The new X-ray absorption fine-structure beamline with sub-second time resolution at the Taiwan Photon Source*," J. Synchrotron Radiat., vol. 28, pp. 930-938, (2021).

[2]. G. Dalba, P. Fornasini, M. Grazioli, "*Local disorder in crystalline and amorphous germanium*," Phys. Rev. B, vol. 52, no. 15, pp. 11034-11043, (1995).

[3]. P. A. Lee, P. H. Citrin, P. Eisenberger, B. M. Kincaid, "*Extended x-ray absorption fine structure - its strengths and limitations as a structural tool*," Rev. Mod. Phys., vol. 53, pp. 769-806, (1981).

[4]. I. V. Pirog, T. I. Nedoseikina, "*Study of effective pair potentials in cubic metals*," Physica B, vol. 334, pp. 123-129, (2003).

[5]. E. Lassner, W. D. Schubert, E. Lüderitz, H. U. Wolf, "*Tungsten, Tungsten alloys, and Tungsten Compounds*," Wiley-VCH, Weinheim, (2000).

[6]. K. Turrell, "*Tungsten (Elements)*," Benchmark Books, New York, (2004).

[7]. N. V. Hung, T. S. Tien, N. B. Duc, D. Q. Vuong, "*High-order expanded XAFS Debye-Waller factors of HCP crystals based on classical anharmonic correlated Einstein model*," Modern Physics Letters B, vol. 28, no. 21, p. 1450174, (2014).

[8]. T. S. Tien, "*Temperature-dependent EXAFS Debye-Waller factor of distorted HCP crystals*," Journal of the Physical Society of Japan, vol. 91, no. 5, pp. 054703, (2022).

[9]. T. S. Tien et al., "*High-order EXAFS cumulants of diamond crystals based on a classical anharmonic correlated Einstein model*," Journal of Physics and Chemistry of Solids, vol. 134, pp. 307-312, (2019).

[10]. N. V. Hung, T. T. Hue, H. D. Khoa, D. Q. Vuong, "*Anharmonic correlated Debye model high-order expanded interatomic effective potential and Debye-Waller factors of bcc crystals*," Physica B, vol. 503, pp. 174-178, (2016).

[11]. G. Bunker, "*Application of the ratio method of EXAFS analysis to disordered systems*," Instruments and Methods in Physics Research, vol. 207, no. 3, pp. 437-444, (1983).

[12]. T. Yokoyama, K. Kobayashi, T. Ohta, A. Ugawa, "*Anharmonic interatomic potentials of diatomic and linear triatomic molecules studied by extended X-ray absorption fine structure*," Physical Review B, vol. 53, no. 10, pp. 6111-6122, (1996).

[13]. R. Freund, R. Ingalls, E. D. Crozier, "*Extended x-ray-absorption fine-structure study of copper under high pressure*," Phys. Rev. B, vol. 39, no. 17, pp. 537-547, (1989).

[14]. L. A. Girifalco, V. G. Weizer, "*Application of the Morse potential function to cubic metals*," Physical Review, vol. 114, no. 3, pp. 687-690, (1959).

[15]. S. H. Simon, "*The Oxford solid state basics*," 1st ed., Oxford University Press, Oxford, (2013).

[16]. N. V. Hung, J. J. Rehr, "*Anharmonic correlated Einstein-model Debye-Waller factors*," Physical Review B, vol. 56, no. 1, pp. 43-46, (1997).

[17]. E. A. Stern, P. Livins, Z. Zhang, "*Thermal vibration and melting from a local perspective*," Phys. Rev. B, vol. 43, no. 11, pp. 8850-8860, (1991).
[18]. N. W. Ashcroft, N. D. Mermin, "*Solid state physics*," 1st ed., Holt-Rinehart & Winston, New York, (1976).

TÓM TẮT

Các cumulant bậc cao của Vônfram trong lý thuyết EXAFS phi điều hoà được tính toán bằng mô hình Einstein tương quan

Các cumulant của cấu trúc tinh tế phổ hấp thụ tia X (EXAFS) phi điều hoà của vônfram (W) trong khai triển đến bậc 4 được tính toán dưới ảnh hưởng của rối loạn nhiệt. Sự phụ thuộc vào nhiệt độ của EXAFS cumulant đã được tính toán tường minh và đơn giản từ một mô hình lý thuyết phát triển dựa trên hàm thế hiệu dụng phi điều hoà và lý thuyết thống kê cổ điển trong mô hình Einstein tương quan. Các tham số nhiệt động của W đã xem xét đến ảnh hưởng của các nguyên tử lân cận gần nhất lên các nguyên tử tán xạ ngược và hấp thụ. Kết quả tính số thu được của W ở các nhiệt độ từ 0 đến 800 K phù hợp với các kết quả thu được từ thực nghiệm và mô hình Debye tương quan phi điều hoà (ACD) ở các nhiệt độ khác nhau. Kết quả này chỉ ra rằng mô hình lý thuyết hiện tại có thể phân tích hữu ích các dữ liệu thực nghiệm của W và các kim loại tương tự khác.

Từ khoá: Các cumulant EXAFS bậc cao; Rối loạn nhiệt; Kim loại vônfram; Thống kê cổ điển; Mô hình Einstein tương quan.